JRAEE
Journal of Robotics, Automation, and Electronics Engineering
Vol. 3, No. 2, 2025, pp. 214-225
e-ISSN 3025-3780
https://journal.uny.ac.id/v3/jraee

Design and Experimental Validation of LQR-Based Altitude Regulation for a Tricopter UAV

Agus Setyo Adi Saputro[a,1], Oktaf Agni Dhewa[b,2,*]

[a,b]Dept. of Electrical and Electronics Engineering, Vocational Faculty, Universitas Negeri Yogyakarta
[1]agussetyo.2020@student.uny.ac.id; [2]oktafagnidhewa@uny.ac.id
[*]Corresponding Author

ARTICLE INFO

Article History
Received 11 Aug 2025
Revised 29 Aug 2026
Accepted 31 Aug 2026

Keywords
Tricopter;
Unmanned Aerial Vehicle;
Altitude Hold;
Linear Quadratic Regulator;
Disturbance Rejection.

ABSTRACT

Altitude regulation is essential for maintaining stable hovering and supporting autonomous operation in tricopter unmanned aerial vehicles (UAVs), whose asymmetric propulsion and rear-rotor tilt mechanism introduce additional control challenges. This study designs, implements, and experimentally evaluates a Linear Quadratic Regulator (LQR)-based altitude-hold controller for a Y-configured tricopter equipped with an inertial sensing module and a downward-facing ultrasonic range sensor for low-altitude feedback. Attitude stabilization was first evaluated using an indoor tuning rig before the complete system was tested under actual flight conditions. The altitude controller was evaluated at reference altitudes of 0.40, 0.85, and 1.25 m and under intentional downward disturbances at a reference altitude of 1.25 m. Across five disturbance trials, the system achieved a mean rise time of 0.513 ± 0.223 s, a mean settling time of 1.113 ± 0.313 s, and a mean steady-state error of 0.0344 ± 0.0069 m. Overshoot occurred in three trials and remained between 1.39% and 1.56%. Without intentional disturbances, steady-state errors of 0.0115, 0.0233, and 0.0064 m were obtained at reference altitudes of 0.40, 0.85, and 1.25 m, respectively. These results demonstrate that the proposed controller can maintain low-altitude hovering and recover from external vertical disturbances within the predefined performance requirements of the tested tricopter platform.

ABSTRAK

Kendali ketinggian merupakan bagian penting dalam mempertahankan kestabilan saat melayang (hovering) dan mendukung pengembangan sistem terbang otonom pada unmanned aerial vehicle (UAV) jenis tricopter. Konfigurasi propulsi yang tidak simetris serta mekanisme kemiringan rotor belakang pada tricopter menimbulkan tantangan tambahan dalam perancangan sistem kendali. Penelitian ini merancang, mengimplementasikan, dan mengevaluasi secara eksperimental sistem kendali altitude hold berbasis Linear Quadratic Regulator (LQR) pada tricopter berkonfigurasi Y yang dilengkapi modul sensor inersial dan sensor ultrasonik yang diarahkan ke permukaan tanah sebagai umpan balik ketinggian rendah. Kestabilan attitude terlebih dahulu diuji menggunakan indoor tuning rig, kemudian sistem secara keseluruhan dievaluasi melalui pengujian terbang. Kendali ketinggian diuji pada referensi 0,40, 0,85, dan 1,25 m serta pada kondisi gangguan vertikal yang diberikan secara sengaja pada ketinggian referensi 1,25 m. Dari lima kali pengujian dengan gangguan, diperoleh rata-rata rise time sebesar 0,513 ± 0,223 s, settling time sebesar 1,113 ± 0,313 s, dan steady-state error sebesar 0,0344 ± 0,0069 m. Overshoot terjadi pada tiga pengujian dengan nilai antara 1,39% hingga 1,56%. Pada pengujian tanpa gangguan yang disengaja, diperoleh steady-state error sebesar 0,0115, 0,0233, dan 0,0064 m masing-masing pada ketinggian referensi 0,40, 0,85, dan 1,25 m. Hasil tersebut menunjukkan bahwa sistem kendali yang dikembangkan mampu mempertahankan kondisi melayang pada ketinggian rendah dan memulihkan posisi vertikal setelah mengalami gangguan dalam batas kinerja yang telah ditentukan pada platform tricopter yang diuji.

1. Introduction

Unmanned aerial vehicles (UAVs) have become important aerial platforms because of their ability to perform remote and autonomous operations in environments that may be difficult, costly, or hazardous for conventional systems. Recent developments have expanded UAV applications across remote sensing, infrastructure inspection, precision agriculture, logistics, surveillance, and emergency response [1]. As UAV applications become increasingly autonomous, reliable flight-control systems capable of maintaining stable position and attitude under varying operating conditions remain an important area of research.

Among multirotor UAV configurations, tricopters employ three rotor–propeller units and commonly use a Y-shaped airframe. In a conventional single-tilt configuration, the rear rotor is mechanically tilted to generate yaw control authority. Compared with symmetric four-rotor configurations, this arrangement reduces the number of propulsion units but introduces asymmetric actuation and additional coupling between thrust-vectoring and rotational dynamics. These characteristics make the tricopter an interesting platform for studying modeling, control allocation, and flight stabilization [2].

The asymmetric actuation of a tricopter can increase coupling among attitude and translational dynamics, particularly when the rear propulsion unit changes its thrust direction for yaw regulation. Consequently, stable hovering requires not only accurate roll, pitch, and yaw stabilization but also reliable altitude regulation. Recent tricopter research has demonstrated that maintaining stable hovering and trajectory control under model uncertainty and external disturbances remains a nontrivial control problem [2], [3]. The altitude-control subsystem must compensate for vertical deviations while the attitude controller simultaneously redistributes actuator commands to preserve vehicle orientation.

Multirotor UAVs are nonlinear, coupled, and underactuated systems, and a wide range of control methods have therefore been investigated, including proportional–integral–derivative (PID), Linear Quadratic Regulator (LQR), Model Predictive Control (MPC), feedback linearization, and sliding-mode control [4]. Among these methods, LQR provides a systematic state-feedback framework that minimizes a quadratic performance index representing both state deviation and control effort. For UAV applications, LQR controllers are commonly designed from a dynamic model linearized around a nominal operating condition such as hovering. Experimental and numerical studies have demonstrated the feasibility of LQR for multirotor attitude, position, and trajectory regulation [5]–[8].

Despite these advances, recent tricopter research has predominantly focused on dynamic modeling, full-pose regulation, trajectory tracking, or advanced robust-control formulations [2], [3]. Experimental investigations focusing specifically on low-altitude hovering using a computationally lightweight state-feedback controller implemented on a low-cost embedded tricopter platform remain comparatively limited. Such implementations are relevant for small UAV systems because stable flight must be achieved using restricted onboard computational resources and relatively inexpensive sensors while maintaining acceptable transient response and disturbance-rejection capability.

Accordingly, this study aims to design, implement, and experimentally evaluate an LQR-based altitude-hold control system on a physical tricopter UAV. The controller is implemented on an embedded flight controller

Journal of Robotics, Automation, and Electronics Engineering
Vol. 3, No. 2, 2025, pp. 214-225
ISSN 3025-3780 (online)
ISSN 3025-4590 (printed)

and evaluated through attitude-stabilization tests, low-altitude hovering at multiple reference heights, and intentional disturbance-rejection experiments. The system performance is characterized using rise time, settling time, overshoot, and steady-state error to evaluate the transient response, steady-state accuracy, and disturbance-recovery capability of the proposed control system under real flight conditions.

2. Research Method

2.1 System Architecture Design

The hardware architecture of the tricopter is shown in Fig. 1. A four-cell (4S) battery with an operating voltage of approximately 14.8–16.8 V supplies the propulsion system and onboard electronics. The battery is connected directly to the three electronic speed controllers (ESCs), while a 5 V/3 A Universal Battery Elimination Circuit (UBEC) supplies the flight controller, inertial sensing module, altitude sensor, receiver, telemetry module, and rear-rotor servo.

A Teensy 3.5 microcontroller serves as the onboard flight controller. It acquires inertial measurements through the I²C interface, reads altitude information from the downward-facing HC-SR04 ultrasonic sensor, receives pilot commands from the radio-control receiver, and executes the attitude and altitude control algorithms in real time. The resulting control commands are converted into pulse-width modulation (PWM) signals for the three ESCs and the rear-rotor tilt servo. Flight and sensor data are simultaneously transmitted to the Ground Control Station (GCS) through a serial telemetry interface for monitoring and data logging.

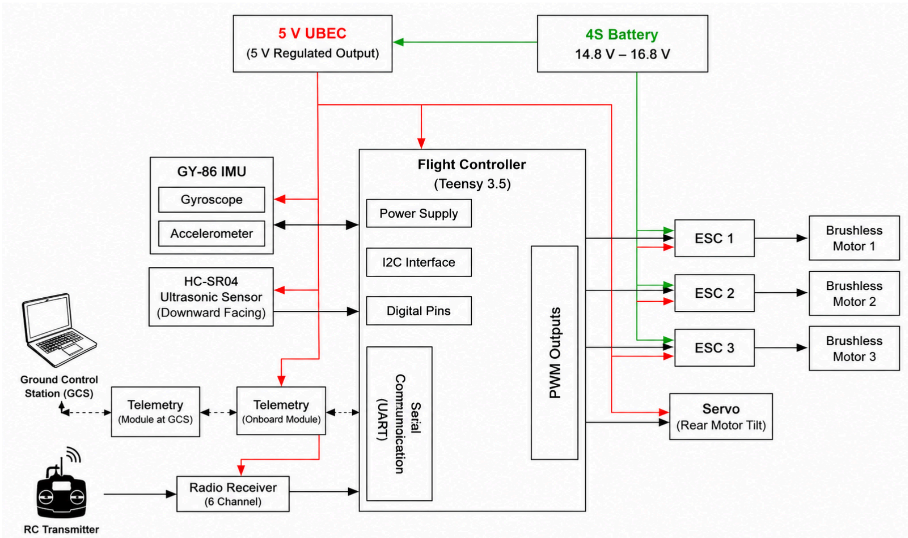

Fig. 1 System architecture design

2.2 Mechanical Design

The experimental tricopter employs a Y-shaped configuration with an angular separation of 120° between the three arms, as shown in Fig. 2. The central frame and rear-rotor tilt mechanism were fabricated from PLA+ using additive manufacturing, while commercially available F450 ABS arms with an approximate physical length of 220 mm were used to support the propulsion units. The rear propulsion unit is mounted on a servo-actuated tilt mechanism that changes the direction of the generated thrust to provide yaw-control authority.

The onboard electronic components are distributed around the central frame to maintain a compact mechanical configuration. The flight controller, inertial sensing module, and telemetry module are installed in the upper compartment, whereas the battery, power-distribution components, receiver, and UBEC are positioned in the middle compartment. The ESCs for the two front propulsion units are mounted beneath the frame. The rear arm accommodates the tilt mechanism, servo motor, and ESC, while the downward-facing ultrasonic sensor is mounted beneath the vehicle with an unobstructed sensing direction toward the ground surface.

Fig. 2 Mechanical design

2.3 Electronic Design

The electronic system is built around a Teensy 3.5 microcontroller, as illustrated in Fig. 3. A GY-86 inertial sensing module is connected to the microcontroller through the I²C communication interface and provides gyroscope and accelerometer measurements for attitude estimation and stabilization. The HC-SR04 ultrasonic sensor is connected through digital trigger and echo lines and is used to measure the distance between the vehicle and the ground during low-altitude operation.

Pilot commands are received through an FS-iA6B six-channel radio receiver. A serial telemetry module provides bidirectional communication between the flight controller and the Ground Control Station for controller tuning, monitoring, and experimental data logging. The Teensy generates PWM outputs for the three ESCs and the rear tilt servo, allowing the flight-control algorithm to independently regulate propulsion thrust and the rear-rotor orientation.

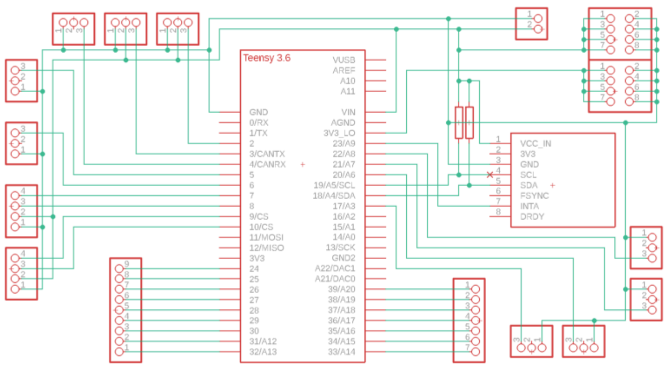

Fig. 3 Electronic design

2.4 Program Flowchart Design

The flight-control software was implemented in C++ on the Teensy 3.5 using the Arduino development environment. The program integrates sensor acquisition, signal filtering, flight-mode management, attitude and altitude control, actuator command generation, and telemetry within the main control loop.

As illustrated in Fig. 4, the program begins by initializing the required variables, communication interfaces, sensors, radio receiver, telemetry module, motors, and rear tilt servo. After initialization, the controller continuously monitors the flight command. When a valid flight command is detected, inertial and altitude measurements are acquired and processed before being supplied to the corresponding control algorithms.

The attitude-control subsystem continuously regulates the roll, pitch, and yaw motions of the tricopter. When altitude-hold mode is activated, the altitude measurement is additionally processed as feedback for the vertical-control subsystem. When altitude-hold mode is inactive, altitude information continues to be acquired for monitoring purposes, but no automatic vertical correction is applied.

The outputs of the attitude and altitude controllers are subsequently converted into PWM commands for the three brushless propulsion motors and the rear tilt servo. Relevant sensor measurements, controller variables, and actuator commands are transmitted to the GCS through the telemetry interface for real-time monitoring and experimental data recording.

Journal of Robotics, Automation, and Electronics Engineering
Vol. 3, No. 2, 2025, pp. 214-225
ISSN 3025-3780 (online)
ISSN 3025-4590 (printed)

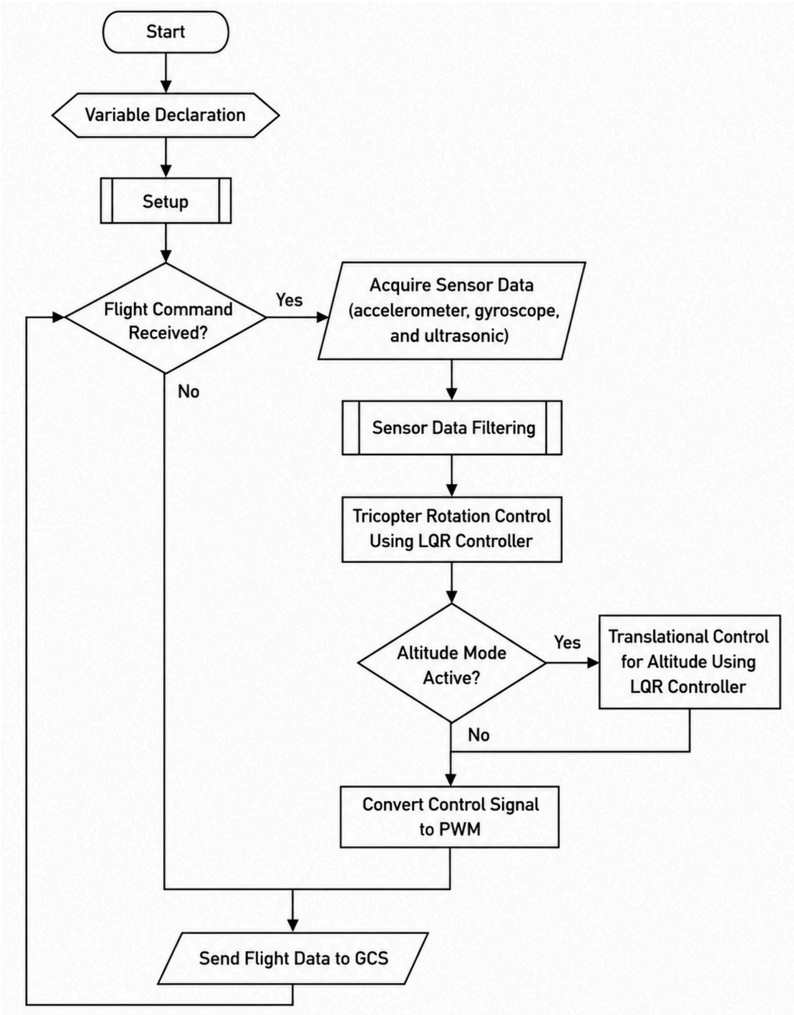

Fig. 4 Program flowchart design

2.1 Control System Design

The tricopter control architecture consists of an attitude-stabilization subsystem for roll, pitch, and yaw regulation and an altitude-control subsystem for vertical-position regulation, as illustrated in Fig. 5. The GY-86 inertial sensing module provides angular-motion information for the attitude controller, while the downward-facing HC-SR04 sensor provides altitude measurements relative to the ground surface. For low-altitude hovering, the vertical dynamics of a multirotor UAV can be expressed as,

$$m\ddot{z} = T\cos(\phi)\cos(\theta) - mg \tag{1}$$

where m is the total mass of the tricopter, z is the vertical position, T is the total thrust generated by the three propulsion units, g is the gravitational acceleration, while φ and θ denote the roll and pitch angles, respectively. During hovering, the tricopter operates close to its equilibrium condition, where the roll and pitch angles are relatively small. Therefore,

$$\cos(\phi) \approx 1, \qquad \cos(\theta) \approx 1 \tag{2}$$

and the nominal thrust required to maintain hovering can be approximated as:

$$T_0 = mg \tag{3}$$

Considering a small deviation from the hovering equilibrium, the vertical dynamics can therefore be simplified as:

$$\Delta\ddot{z} = \frac{\Delta T}{m} \tag{4}$$

where ΔT represents the variation in total thrust relative to the nominal hover thrust. For altitude regulation, the altitude error is defined as:

$$e_z = z - z_{\text{ref}} \tag{5}$$

where *z_ref* represents the desired altitude. The state vector of the altitude-control subsystem is then defined as:

$$x_z = [e_z \quad \dot{z}]^T \tag{6}$$

where $\dot{z}$ represents the vertical velocity of the tricopter. Based on the linearized vertical dynamics, the altitude subsystem can be represented in state-space form as:

$$\dot{x}_z = A_z x_z + B_z u \tag{7}$$

with:

$$A_z = \begin{bmatrix} 0 & 1 \\ 0 & 0 \end{bmatrix} \tag{8}$$

and:

$$B_z = \begin{bmatrix} 0 \\ \frac{1}{m} \end{bmatrix} \tag{9}$$

where *u* represents the incremental thrust command generated by the altitude controller.

The Linear Quadratic Regulator determines the control input by minimizing a quadratic performance index defined as:

$$J = \int_0^\infty \left(x_z^T Q_z x_z + u^T R_z u \right) dt \tag{10}$$

where Q_z is the state-weighting matrix used to determine the relative importance of altitude error and vertical-velocity error, while R_z is the control-weighting parameter used to penalize excessive control effort.

The corresponding state-feedback control law is expressed as:

$$u = -K_z x_z \tag{11}$$

where K_z represents the LQR feedback-gain matrix. The weighting matrices used in the altitude-controller design are:

$$Q_z = \begin{bmatrix} q_1 & 0 \\ 0 & q_2 \end{bmatrix} \tag{12}$$

and:

$$R_z = r \tag{13}$$

The feedback-gain matrix is obtained by solving the Algebraic Riccati Equation (ARE). The resulting altitude-control gain used in the experimental implementation is:

$$K_z = [5.8 \quad 0.68] \tag{14}$$

Thus, the altitude-control command can be expressed explicitly as:

$$u = -5.8 e_z - 0.68 \dot{z} \tag{15}$$

The first feedback term provides corrective action proportional to the altitude error, whereas the second term provides damping based on the vertical velocity. During actual flight, the incremental control command is combined with the nominal hover command before being distributed to the three propulsion units. Therefore, the total vertical-control command can be represented as:

$$u_{\text{total}} = u_{\text{hover}} + u \tag{16}$$

where u_{hover} represents the nominal actuator command required to counteract the vehicle weight during hovering.

For attitude stabilization, LQR controllers were independently designed for the roll, pitch, and yaw axes. The state-weighting matrices were initially evaluated in MATLAB, and the resulting feedback gains were subsequently implemented on the Teensy 3.5 flight controller. The attitude-control subsystem continuously regulates the vehicle orientation, whereas the altitude controller regulates vertical motion when altitude-hold mode is activated.

The HC-SR04 was employed as a low-cost downward-facing range sensor suitable for the low-altitude operating range considered in this study. Because the measured range corresponds to the distance along the

ISSN 3025-3780 (online)
ISSN 3025-4590 (printed)

sensor measurement axis, changes in roll and pitch may introduce deviations between the measured range and the actual vertical altitude. Therefore, the altitude-control experiments were primarily conducted under near-hover conditions in which roll and pitch deviations remained relatively small.

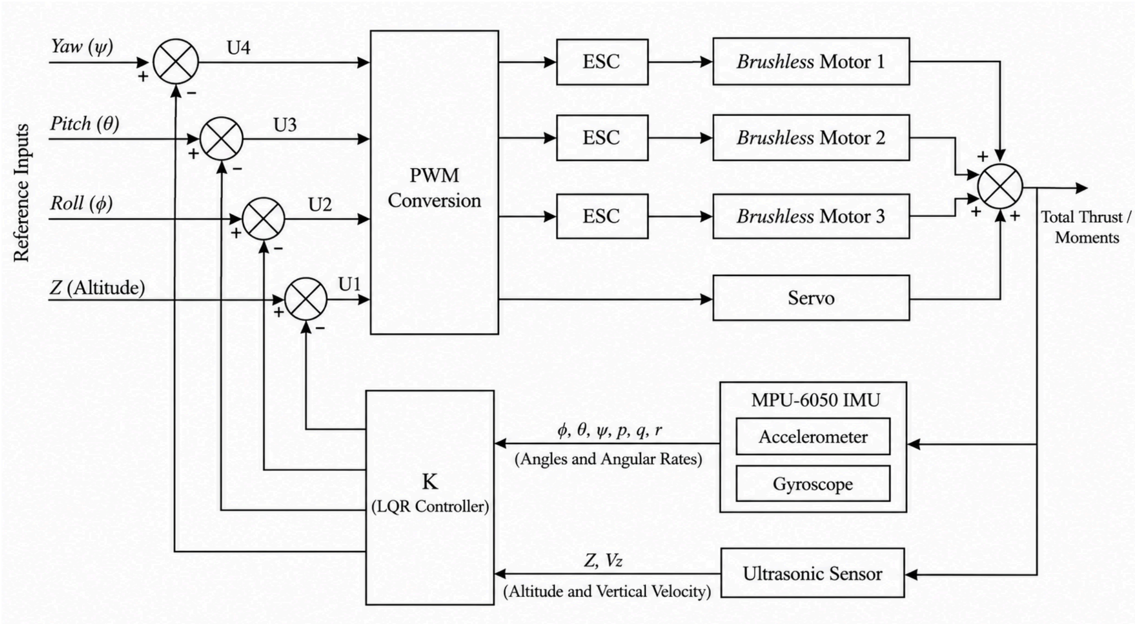

Fig. 5 Control system design

3. Result and Discussion

3.1 Attitude Stabilization Control Testing Using a Tuning Rig

The attitude-control system for the roll, pitch, and yaw axes was first designed and evaluated in MATLAB. The state-weighting matrices were iteratively adjusted while maintaining the control-weighting parameter at (R=1). The selected weighting matrices were (Q=[173,0.1]) for the roll axis, (Q=[168,0.2]) for the pitch axis, and (Q=[178,0.2]) for the yaw axis. The corresponding LQR feedback gains obtained from the MATLAB design are summarized in Table 1.

Table 1. Selected Q, R, and Resulting LQR Gain Matrices for Roll (ϕ), Pitch (θ), and Yaw (ψ)

Axis	$Qmatrix$	R	$Kmatrix$
Roll	$Q_\phi = \begin{bmatrix} 0 & 173 & 0 & 0 & 0 & 0 & 0 & 0 \\ 0 & 0 & 0 & 0 & 0 & 0.1 & 0 & 0 \end{bmatrix}$	$R_\phi = 1$	$K_\phi = \begin{bmatrix} 0 & 13.153 & 0 & 0 & 0 & 0 & 0 & 0 \\ 0 & 0 & 0 & 0 & 0 & 0.431 & 0 & 0 \end{bmatrix}$
Pitch	$Q_\theta = \begin{bmatrix} 0 & 0 & 168 & 0 & 0 & 0 & 0 & 0 \\ 0 & 0 & 0 & 0 & 0 & 0 & 0.2 & 0 \end{bmatrix}$	$R_\theta = 1$	$K_\theta = \begin{bmatrix} 0 & 0 & 12.961 & 0 & 0 & 0 & 0 & 0 \\ 0 & 0 & 0 & 0 & 0 & 0 & 0.633 & 0 \end{bmatrix}$
Yaw	$Q_\psi = \begin{bmatrix} 0 & 0 & 0 & 178 & 0 & 0 & 0 & 0 \\ 0 & 0 & 0 & 0 & 0 & 0 & 0 & 0.2 \end{bmatrix}$	$R_\psi = 1$	$K_\psi = \begin{bmatrix} 0 & 0 & 0 & 13.342 & 0 & 0 & 0 & 0 \\ 0 & 0 & 0 & 0 & 0 & 0 & 0 & 0.646 \end{bmatrix}$

The resulting gains were subsequently implemented on the physical tricopter and evaluated using an indoor tuning rig. Five repeated experiments were conducted for each axis to evaluate the repeatability of the transient and steady-state responses.

3.2 Roll axis response

The roll-axis test results are summarized in Table 2 and the representative response is shown in Fig. 6. Across five trials, the controller achieved a mean rise time of 0.434 ± 0.276 s, a mean settling time of 1.400 ± 1.655 s, and a mean steady-state error of 0.526 ± 0.594°. Overshoot was observed in only one trial, reaching 4.58°.

The relatively large dispersion in settling time was primarily influenced by Trial 4, which required 4.33 s to satisfy the settling criterion. In contrast, the remaining trials exhibited considerably shorter settling times. This variation indicates that although the controller maintained roll stability, the transient response remained sensitive to experimental disturbances, mechanical variations, or interaction with the tuning rig.

Table 2. Roll Test Results Using Tuning Rig

Response	Test 1	Test 2	Test 3	Test 4	Test 5
Rise time (s)	0.50	0.17	0.50	0.17	0.83
Settling time (s)	0.67	0.33	0.67	4.33	1.00
Overshoot (°)	-	-	-	4.58	-
SS Error (°)	0.04	0.13	0.19	0.85	1.42

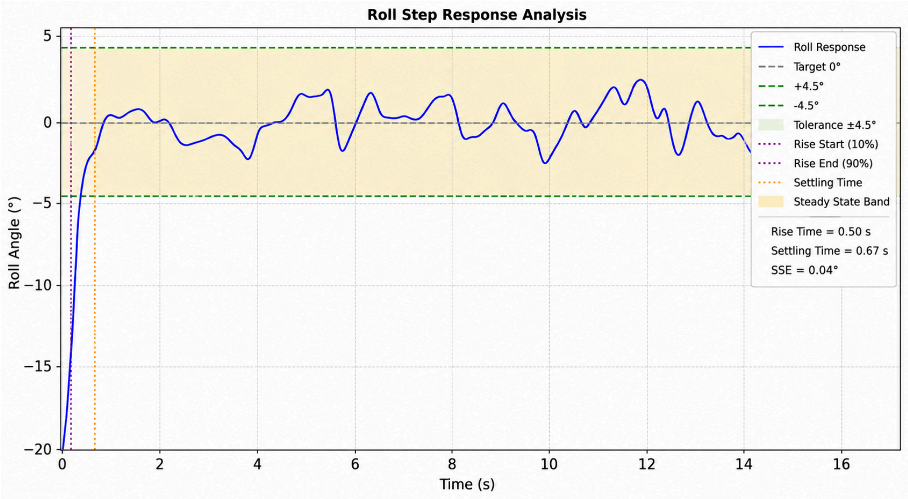

Fig. 6 Roll axis response using the tuning rig

3.3 Pitch axis response

The pitch-axis results are presented in Table 3 and Fig. 7. Across the five experiments, the controller produced a mean rise time of 0.800 ± 0.988 s, a mean settling time of 1.568 ± 1.131 s, and a mean steady-state error of 0.598 ± 0.470°.

The relatively high variation in rise time was mainly associated with Trial 3, which required 2.50 s compared with considerably shorter values in the other experiments. A positive overshoot of 4.62° was observed in Trial 2, while Trial 5 exhibited a deviation in the opposite direction. Overall, the experimental results indicate that the pitch controller was capable of maintaining stable angular regulation, although variations in transient response remained evident among repeated trials.

Table 3. Pitch Test Results Using Tuning Rig

Response	Test 1	Test 2	Test 3	Test 4	Test 5
Rise time (s)	0.33	0.17	2.50	0.17	0.83
Settling time (s)	0.50	1.67	2.67	0.33	2.67
Overshoot (°)	-	4.62	-	-	-4.56
SS Error (°)	1.27	0.19	0.11	0.67	0.75

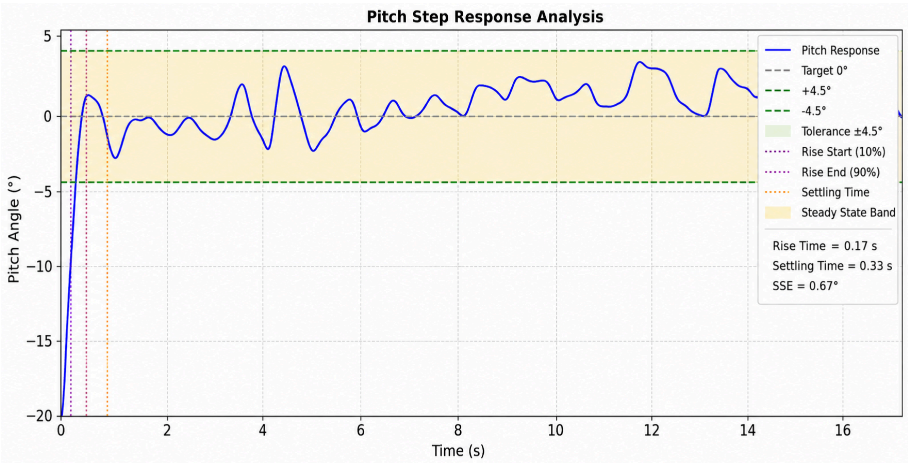

ISSN 3025-3780 (online)
ISSN 3025-4590 (printed)

Fig. 7. Pitch axis response using the tuning rig

3.4 Yaw axis response

The yaw-axis results are summarized in Table 4 and illustrated in Fig. 8. Across five trials, the controller achieved a mean rise time of 0.798 ± 0.493 s, a mean settling time of 1.000 ± 0.514 s, and a mean steady-state error of 0.740 ± 0.563°. No overshoot was observed during the five experiments.

Although stable yaw responses were consistently achieved, differences in steady-state error were observed among repeated trials. In a tricopter configuration, yaw regulation depends directly on the mechanical tilt and thrust generated by the rear propulsion unit. Consequently, the repeatability of the yaw response may also be influenced by servo dynamics, mechanical backlash, thrust variation, and asymmetry of the propulsion system.

Table 4. Yaw Test Results Using Tuning Rig

Response	Test 1	Test 2	Test 3	Test 4	Test 5
Rise time (s)	0.33	1.50	1.00	0.83	0.33
Settling time (s)	0.50	1.67	1.33	1.00	0.50
Overshoot (°)	-	-	-	-	-
SS Error (°)	1.21	0.23	1.22	0.04	1.00

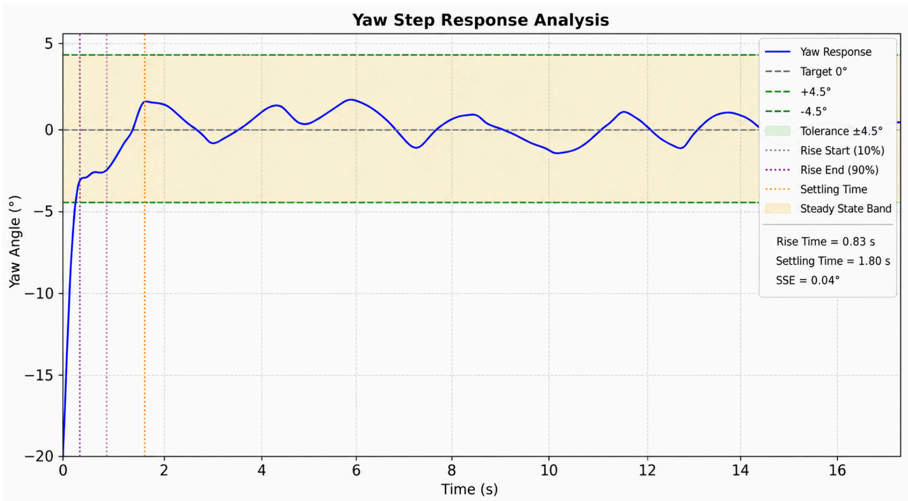

Fig. 8 Yaw axis response using the tuning rig

The tuning-rig experiments therefore demonstrate that the implemented attitude controllers were capable of stabilizing all three rotational axes before the altitude controller was evaluated under free-flight conditions. The results also indicate that repeated experimental measurements provide more representative information about controller performance than an individual best-response trial.

3.5 Altitude Control System Testing with Intentional Disturbances

The altitude-hold controller was experimentally evaluated at a reference altitude of 1.25 m to investigate its ability to recover from vertical disturbances. Five flight trials were conducted. After the tricopter reached approximately steady hovering, an intentional downward displacement of more than 0.20 m was introduced, after which the vehicle was released and allowed to recover autonomously toward the reference altitude.

The altitude response was evaluated in terms of rise time, settling time, overshoot, and steady-state error. The individual results are summarized in Table 5, while a representative altitude response is illustrated in Fig. 9.

Table 5. Altitude-Hold Performance under Intentional Disturbances at 1.25 m

Response	Test 1	Test 2	Test 3	Test 4	Test 5	Minimum Requirement
Rise time (s)	0.521	0.815	0.476	0.562	0.190	< 3s
Settling time (s)	1.224	1.019	1.342	0.611	1.371	< 6s
Overshoot (°)	1.559	-	1.393	-	1.410	±15%
SS Error (°)	0.027	0.029	0.044	0.034	0.038	< 0.125m

Across the five disturbance trials, the controller achieved a mean rise time of 0.513 ± 0.223 s and a mean settling time of 1.113 ± 0.313 s. The mean steady-state error was 0.0344 ± 0.0069 m, corresponding to approximately 2.75% of the 1.25 m reference altitude.

Overshoot occurred in three of the five trials and ranged from approximately 1.39% to 1.56%, while no overshoot was observed in the remaining two trials. All measured rise-time, settling-time, overshoot, and steady-state-error values remained within the predefined performance requirements listed in Table 5.

These experimental results demonstrate that the implemented controller was able to restore the tricopter toward its reference altitude after the applied downward perturbations. However, because the disturbance was introduced manually and only one nominal altitude was evaluated in this experiment, the results should be interpreted as evidence of disturbance-rejection capability under the tested conditions rather than as a general proof of robustness against arbitrary disturbances.

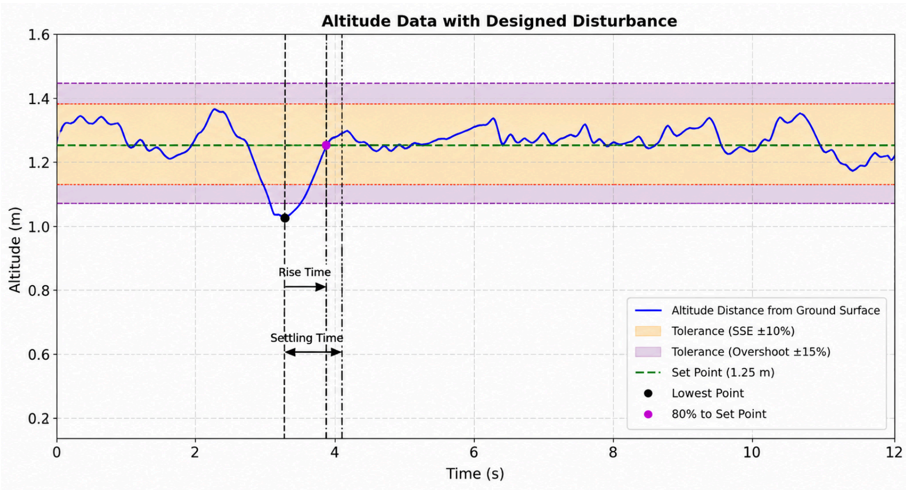

Fig. 9 Altitude response at 1.25 m under intentional disturbance

3.6 Altitude Control System Testing without Intentional Disturbance

The altitude-hold controller was further evaluated at reference altitudes of 0.40, 0.85, and 1.25 m without intentionally applied external disturbances. The same controller configuration was maintained for all three setpoints to evaluate whether a single feedback-gain configuration could regulate altitude across the investigated low-altitude operating range.

After the vehicle reached each reference altitude, altitude measurements were recorded during a 10 s steady-hover interval. The corresponding responses are illustrated in Fig. 10.

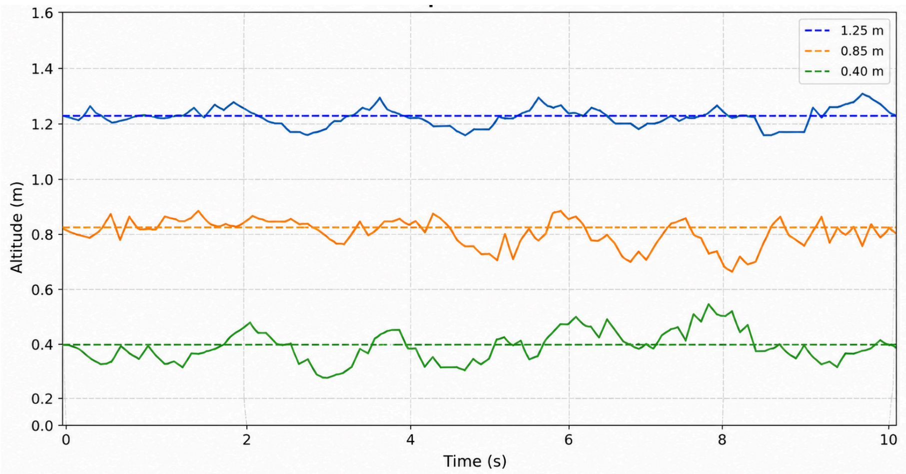

Fig. 10 Altitude response at multiple setpoints

The measured steady-state errors were 0.0115 m, 0.0233 m, and 0.0064 m at reference altitudes of 0.40, 0.85, and 1.25 m, respectively. These values correspond to relative errors of approximately 2.88%, 2.74%, and 0.51% of the respective altitude references.

Among the investigated operating points, the 1.25 m reference altitude exhibited the lowest observed absolute and relative steady-state error. Nevertheless, the error did not vary monotonically with altitude, as the 0.85 m condition produced a larger error than both the lower and higher reference altitudes. This behavior may be associated with ultrasonic measurement variability, local airflow interaction, ground-reflection characteristics, or differences in the flight condition during each test.

The results indicate that the same controller configuration was capable of maintaining hovering across the investigated reference altitudes. However, repeated experiments at each altitude and longer-duration tests would be required to determine statistically whether controller performance is significantly dependent on operating altitude.

4. Conclusion

This study designed, implemented, and experimentally evaluated an LQR-based altitude-hold control system on a physical tricopter UAV. Attitude stabilization was first evaluated using an indoor tuning rig for the roll, pitch, and yaw axes before the complete altitude-control system was tested under actual flight conditions.

During intentional downward disturbances at a reference altitude of 1.25 m, five flight trials produced a mean rise time of 0.513 ± 0.223 s, a mean settling time of 1.113 ± 0.313 s, and a mean steady-state error of 0.0344 ± 0.0069 m. Overshoot occurred in three trials but remained below 1.6%. All measured performance parameters satisfied the predefined experimental requirements under the tested conditions.

Additional altitude-hold experiments at reference altitudes of 0.40, 0.85, and 1.25 m produced steady-state errors of 0.0115, 0.0233, and 0.0064 m, respectively. The corresponding relative errors were approximately 2.88%, 2.74%, and 0.51%. The results demonstrate that a single controller configuration can maintain low-altitude hovering across the investigated operating range, with the smallest observed error occurring at the 1.25 m reference altitude.

The current evaluation is limited by the use of a single downward-facing ultrasonic sensor, relatively short steady-hover measurements, and manually applied disturbance inputs. Future work should therefore investigate repeated and standardized disturbance experiments, longer-duration free-flight evaluations, and altitude estimation based on multi-sensor fusion. Combining inertial and barometric measurements with a downward-facing time-of-flight or laser range sensor may improve altitude estimation under varying ground surfaces and operating conditions [9]. Integral augmentation of the LQR structure may also be investigated to further reduce persistent steady-state tracking errors.

Author Contribution:

All authors contributed equally as main contributors to this paper. All authors read and approved the final paper.

Funding:

This research received no external funding.

Conflicts of Interest:

The authors declare no conflict of interest.

References

[1] K. Telli, O. Kraa, Y. Himeur, A. Ouamane, M. Boumehraz, S. Atalla, and W. Mansoor, "A comprehensive review of recent research trends on unmanned aerial vehicles (UAVs)," *Systems*, vol. 11, no. 8, Art. no. 400, 2023, doi: 10.3390/systems11080400.

[2] M. Ramp and E. Papadopoulos, "On modeling and control of a holonomic tricopter," *Journal of Intelligent & Robotic Systems*, vol. 105, Art. no. 51, 2022, doi: 10.1007/s10846-021-01541-9.

[3] D. Abara, P. Bhowmick, and A. Lanzon, "A negative imaginary robust formation control scheme for networked multi-tilt tricopters utilizing an inner-loop sliding-mode control technique," *Automatica*, vol. 169, Art. no. 111813, 2024, doi: 10.1016/j.automatica.2024.111813.

[4] M. Rinaldi, S. Primatesta, and G. Guglieri, "A comparative study for control of quadrotor UAVs," *Applied Sciences*, vol. 13, no. 6, Art. no. 3464, 2023, doi: 10.3390/app13063464.

[5] M. Okasha, J. Kralev, and M. Islam, "Design and experimental comparison of PID, LQR and MPC

stabilizing controllers for Parrot Mambo mini-drone," *Aerospace*, vol. 9, no. 6, Art. no. 298, 2022, doi: 10.3390/aerospace9060298.

[6] B. M. Nguyen, T. Kobayashi, K. Sekitani, M. Kawanishi, and T. Narikiyo, "Altitude control of quadcopters with absolute stability analysis," *IEEJ Journal of Industry Applications*, vol. 11, no. 4, pp. 562–572, 2022.

[7] J. Madeiras, C. Cardeira, and P. Oliveira, "Trajectory tracking of a quadrotor via full-state feedback control," *Aerospace Science and Technology*, vol. 147, Art. no. 109013, 2024, doi: 10.1016/j.ast.2024.109013.

[8] A. Sir Elkhatem and S. N. Engin, "Robust LQR and LQR-PI control strategies based on adaptive weighting matrix selection for a UAV position and attitude tracking control," *Alexandria Engineering Journal*, vol. 61, no. 8, pp. 6275–6292, 2022, doi: 10.1016/j.aej.2021.11.057.

[9] V. Pritzl, M. Vrba, C. Tortorici, R. Ashour, and M. Saska, "Adaptive estimation of UAV altitude in complex indoor environments using degraded and time-delayed measurements with time-varying uncertainties," *Robotics and Autonomous Systems*, vol. 160, Art. no. 104315, 2023, doi: 10.1016/j.robot.2022.104315.